# NAVAL POSTGRADUATE SCHOOL
# Monterey, California


# THESIS



A COMPARISON OF THE AGING KINETICS
OF A CAST ALUMINA-6061 ALUMINUM COMPOSITE
AND A MONOLITHIC 6061 ALUMINUM ALLOY

by

Johanna L. Hafley

December 1989

Thesis Advisor: PROFESSOR I. DUTTA

# REPORT DOCUMENTATION PAGE

Form Approved
OMB No 0704-0188

| | |
|---|---|
| 1a REPORT SECURITY CLASSIFICATION<br>UNCLASSIFIED | 1b RESTRICTIVE MARKINGS |
| 2a SECURITY CLASSIFICATION AUTHORITY | 3 DISTRIBUTION / AVAILABILITY OF REPORT<br>Approved for public release; distribution is unlimited |
| 2b DECLASSIFICATION / DOWNGRADING SCHEDULE | |
| 4 PERFORMING ORGANIZATION REPORT NUMBER(S) | 5 MONITORING ORGANIZATION REPORT NUMBER(S) |
| 6a NAME OF PERFORMING ORGANIZATION<br>Naval Postgraduate School<br>6b OFFICE SYMBOL (If applicable)<br>Code 69 | 7a NAME OF MONITORING ORGANIZATION |
| 6c ADDRESS (City, State, and ZIP Code)<br>Monterey, California 93942-5000 | 7b ADDRESS (City, State, and ZIP Code) |
| 8a NAME OF FUNDING / SPONSORING ORGANIZATION<br>8b OFFICE SYMBOL (If applicable) | 9 PROCUREMENT INSTRUMENT IDENTIFICATION NUMBER |
| 8c ADDRESS (City, State, and ZIP Code) | 10 SOURCE OF FUNDING NUMBERS<br>PROGRAM ELEMENT NO / PROJECT NO / TASK NO / WORK UNIT ACCESSION NO |

11 TITLE (Include Security Classification)
A COMPARISON OF THE AGING KINETICS OF A CAST ALUMINA-6061 ALUMINUM COMPOSITE AND A MONOLITHIC 6061 ALUMINUM ALLOY

12 PERSONAL AUTHOR(S)
Johanna L. Hafley

| 13a TYPE OF REPORT | 13b TIME COVERED FROM _____ TO _____ | 14 DATE OF REPORT (Year, Month, Day) | 15 PAGE COUNT |
|---|---|---|---|
| | | December 1989 | 62 |

16 SUPPLEMENTARY NOTATION
The views expressed in this thesis are those of the author and do not reflect the official policy or position of the Department of Defense or the U.S. Government.

| 17 COSATI CODES | | | 18 SUBJECT TERMS (Continue on reverse if necessary and identify by block number) |
|---|---|---|---|
| FIELD | GROUP | SUB-GROUP | aluminum composite |
| | | | |
| | | | |

19 ABSTRACT (Continue on reverse if necessary and identify by block number)

Electrical resistivity and hardness measurements were conducted during isothermal aging treatments of an alumina particulate reinforced 6061 aluminum metal matrix composite and a monolithic 6061 aluminum control material. Transmission electron microscopy was utilized to examine the microstructural changes accompanying the changes in the resistivity of the monolith during aging. In addition, differential scanning calorimetry was used to investigate the growth kinetics and thermal stability of the metastable phases in the control sample. From DSC experiments, the heats of formation of the metastable phases were determined as functions of aging time and temperature. These results were used to characterize the aging behavior of the matrix material.

| | |
|---|---|
| 20 DISTRIBUTION / AVAILABILITY OF ABSTRACT<br>☒ UNCLASSIFIED/UNLIMITED ☐ SAME AS RPT ☐ DTIC USERS | 21 ABSTRACT SECURITY CLASSIFICATION<br>Unclassified |
| 22a NAME OF RESPONSIBLE INDIVIDUAL<br>I. Dutta, Professor | 22b TELEPHONE (Include Area Code)<br>(408) 646-2581<br>22c OFFICE SYMBOL<br>69Du |

Approved for public release; distribution is unlimited.

# A Comparison of the Aging Kinetics of a Cast Alumina-6061 Aluminum Composite and a Monolithic 6061 Aluminum Alloy

by

Johanna L. Hafley
Lieutenant, United States Navy
B.S., Pennsylvania State University, 1980

Submitted in partial fulfillment
of the requirements for the degree of

MASTER OF SCIENCE IN MECHANICAL ENGINEERING

from the
NAVAL POSTGRADUATE SCHOOL
December 1989

**ABSTRACT**

Electrical resistivity and hardness measurements were conducted during isothermal aging treatments of an alumina particulate reinforced 6061 aluminum metal matrix composite and a monolithic 6061 aluminum control material. Transmission electron microscopy was utilized to examine the microstructural changes accompanying the changes in the resistivity of the monolith during aging. In addition, differential scanning calorimetry was used to investigate the growth kinetics and thermal stability of the metastable phases in the control sample. From DSC experiments, the heats of formation of the metastable phases were determined as functions of aging time and temperature. These results were used to characterize the aging behavior of the matrix material.

## TABLE OF CONTENTS

# I. INTRODUCTION

## A. METAL MATRIX COMPOSITES

A metal matrix composite (MMC) is a mixture or combination of a ductile metallic matrix and a more brittle, usually nonmetallic, reinforcement material. The two materials are essentially insoluble in each other. Some of the properties which can be improved by forming a composite material are:

- strength
- stiffness
- wear resistance
- weight
- corrosion resistance
- thermal conductivity

Higher stiffness is one of the most important properties because, unlike strength, stiffness cannot be improved much by alloying or heat treating. This improved property has found interest in many markets. Notably an extruded mountain bike wheel rim of MMC weighs only 427 grams, with no warping and improved stiffness, while the aluminum weighs 450 - 530 grams. Other wrought aluminum MMCs are being

evaluated for a variety of uses such as drive shafts, connecting rods, and rocker arms. [Ref. 1]

## B. ACCELERATED AGING AND MICROSTRUCTURAL EVOLUTION

### 1. Precipitation Hardening

Precipitation hardening (aging) is used to produce a fine, uniform dispersion of a hard precipitate in a softer, less brittle matrix. Not all alloys are age hardenable. In order to be age hardenable the alloy must form a single phase solid solution on heating above the solvus line and then cool to a two-phase region. The matrix must be more ductile than the precipitate. A very rapid cooling (quench) must suppress formation of the second phase producing a supersaturated solid solution. The initial precipitates that form must be at least partially coherent with the matrix structure.

The first step in an age-hardening heat treatment is to solution treat. The alloy must be heated to a temperature above the solvus temperature and held until a homogeneous solid solution is produced. This step dissolves all precipitates. After the solution treatment, the alloy is quenched. This must be done quickly enough that the atoms do not have time to diffuse to potential nucleation sites and permit the precipitate to form. The structure, still a supersaturated solid solution, not at equilibrium

and therefore unstable, is heated to a temperature below the solvus. Because of the instability, the excess solute atoms diffuse to numerous nucleation sites and a precipitate forms and grows. If the alloy is held at the aging temperature for a sufficient time, an equilibrium structure of primary solid solution and precipitate is produced. Natural aging is done at room temperature while artificial aging is done at elevated temperatures.

### 2. Microstructural Evolution in 6061 Aluminum

The details of the precipitation sequence of 6061 aluminum are somewhat controversial. However, the sequence does appear to involve the following [Ref. 2]:

1. supersaturated solid solution
2. vacancy clusters
3. vacancy - silicon clusters
4. vacancy rich coherent Al-Mg-Si Guinier-Preston (GP) zones (needle-shaped)
5. disordered, partially coherent needle shaped phase
6. ordered, partially coherent needle-shaped phase ($\beta''$)
7. semicoherent, hexagonal rod-shaped phase ($\beta'$)
8. equilibrium platelets, $\beta$ or magnesium silicide ($Mg_2Si$).

### 3. Accelerated Aging

Accelerated aging has been observed in many precipitation hardened metal matrix composites, relative to the unreinforced, monolithic alloy. The metal matrix

composites reach peak strength and peak hardness more quickly, as shown in Figure 1 [Ref. 3].

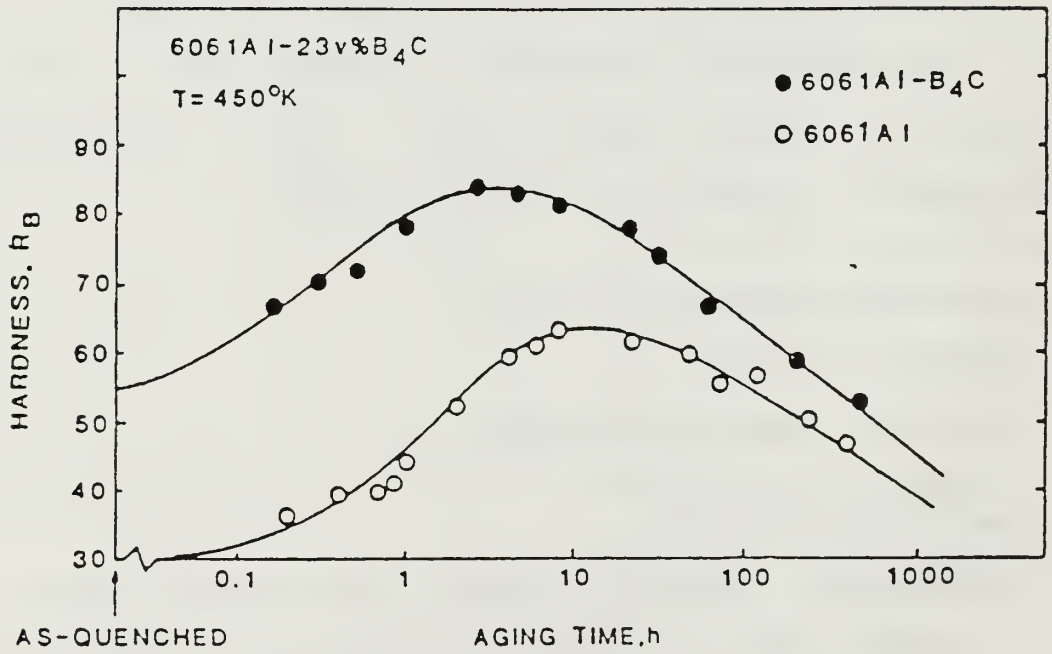


**Figure 1: The variation in matrix microhardness as a function of aging time for the aluminum alloy 2124-SiC composite and the control alloy 2124. The aging temperature is 177°C. [Ref. 3]**

There are two primary theories for the mechanisms of the accelerated aging. The first one is that nucleation and growth are enhanced due to high dislocation density in the immediate vicinity of the reinforcement. The second is that diffusion is enhanced due to thermal residual stresses generated in the matrix due to differential thermal contraction of the reinforcement and matrix materials during cooling from the solutionizing temperature. Much research has been done to identify the operative mechanisms.

Studies by Christman and Suresh [Ref. 4] on 2124-SiC composite indicated that a reason for the accelerated aging of the composite is that dislocations in the matrix of the composite serve as nucleation sites for the formation of precipitates during the aging of the composites. The increase in MMC dislocation density arises during the quench stage of the precipitation heat treatment because of the differences in thermal expansion of the matrix and the reinforcement. The evidence they used included transmission electron microscope (TEM) work which showed an increased dislocation density in the matrix of the composite and preferential nucleation of the strengthening precipitates along dislocation lines during the aging of the composite. This facilitates the attainment of peak matrix hardness at much shorter times than in the control alloy. Their qualitative analysis of nucleation and growth kinetics of the strengthening precipitates for both reinforced and

unreinforced materials shows a shift in nucleation time but not in growth kinetics. They also confirmed that cold work of unreinforced material also produced an accelerated aging effect.

The results of Nieh and Karlak [Ref. 3], who studied $B_4C$ reinforced 6061 aluminum, showed accelerated aging for the composite. As seen in Figure 1, the composite reached peak hardness in about three hours at 450K while a control alloy took ten hours. They attributed this acceleration to the presence of high diffusivity paths in the composite, particularly the dislocations introduced by differential thermal expansion and the particle matrix interfaces.

Suresh, Christman and Sugimura [Ref. 5] studied the aging behavior of cast SiC-aluminum composites and found aging to be accelerated in the composite material. They used six, 13 and 20 volume percent SiC and found that the peak aging times for the three composite materials do not exhibit any significant differences. Their results also implied that the enhanced dislocation densities in the matrices of the composites do not markedly contribute to strengthening despite the pronounced effect on aging. They also found that with no aging the composites and the monolith exhibited essentially the same microhardness in the solutionized and as-quenched condition. Additions of particles beyond six volume percent did not lead to any noticeable enhancements in the matrix dislocation density.

Apparently even six volume percent of SiC particles in the matrix generates a sufficient number of dislocations due to the thermal contraction mismatch for the heterogeneous nucleation of the strengthening precipitates. This observation is at variance with suggestions of possible strengthening in MMCs due to the generation of excess matrix dislocations. Most other findings predict that the composite has a higher solutionized and as-quenched hardness than the matrix material because of the much higher degree of dislocations.

The second explanation for accelerated aging arises from the generation of an elastic residual stress field in the matrix around the reinforcement as a result of quenching. Stresses applied during aging are known to cause rearrangement of precipitates. The basis of stress assisted diffusion is the relief of the total strain energy of the system. If the solute atoms are larger than the matrix atoms, they will move to a region of tensile residual stress, while smaller solute atoms would flow to regions of compressive residual stress.

Dutta and Bourell [Ref. 6] conducted studies to ascertain which mechanism contributes more to accelerated aging. Both mechanisms aid the diffusion of solute atoms, thereby leading to more rapid precipitation. In their work a 6061 aluminum alloy reinforced with 10 volume percent SiC whiskers of variable aspect ratios was studied

experimentally. These results were compared with a control 6061 alloy which was both in the unstrained and strained conditions. It was found that the strained control alloy, with approximately the same expended plastic work as the composite, showed a similar $\beta'$ (transition $Mg_2Si$) precipitation rate and activation energy as the composite. However, the unstrained alloy had a much higher activation energy for precipitation. A theoretical model was developed to predict the rate of precipitation in the residual stress field of the matrix. This rate was compared with the rate of precipitation on a regular edge dislocation array. It was found that, for realistic values of fiber radii and dislocation densities, both mechanisms give comparable precipitation rates. However, solute atoms flowing towards the matrix-fiber interface under the influence of the residual stress field on encountering matrix dislocations are trapped, thereby lowering the activation energy to that of precipitation on dislocations. It was concluded that, for MMCs with large fibers and high dislocation densities, dislocation generation is the principal contributor to accelerated aging, while in MMCs with small fibers and low dislocation densities the residual stress mechanism predominates. For intermediate fiber radii and dislocation densities, both mechanisms could be important. However, in actual MMCs dislocations seem to play the dominant role.

Studies by Papazian [Ref. 7] on SiC reinforced composites with different alloy matrices determined that the overall age-hardening sequence of the alloy was not changed by the addition of the particles, but that the volume fractions of various phases and the precipitation kinetics were substantially modified. Both precipitation and dissolution kinetics were found to be generally accelerated.

## C. RESEARCH OBJECTIVE

Most of the previous work on the aging behavior of precipitation hardenable metal matrix composites reported in the literature has been concentrated on powder metallurgy products. Very recently, however, Suresh, Christman and Sugimura [Ref. 5] studied the aging behavior in cast Al-3.5 weight percent Cu alloy - SiC particulate composites and found the aging to be accelerated in comparison with the monolithic alloy. Papazian's [Ref. 7] work included one cast material, 7475 aluminum reinforced with SiC particulates. So far, no known work has been done to investigate the aging response of cast alumina particle reinforced aluminum matrix composites. The purpose of this work is to study the effect of alumina particle reinforcement on the aging behavior of cast 6061 aluminum matrix composite.

## II. DESCRIPTION OF MATERIALS

The composite used for this thesis work, 6061 aluminum - 15 volume percent alumina, was fabricated by casting at Dural Aluminum Composites Corporation in San Diego, CA. The composite was extruded to homogenize the microstructure and supplied as a 3" x 3/4" bar. The matrix alloy, ingot-grade 6061 aluminum, is made up of aluminum, 0.8-1.2% magnesium and 0.4 - 0.8 % silicon. A proprietary pretreatment, probably a coating, allows chemically active molten aluminum to wet the particles without reacting with and degrading the ceramic. The treatment lessens dissolved gases and impurities and aids uniform particle distribution for consistent mechanical properties throughout the matrix. [Ref. 8]

Figure 2 is a representative microstructure of the as-received composite. As seen in the figure, the alumina particles are irregularly shaped with sharp corners. There is an appreciable degree of clustering of $Al_2O_3$ which led to particle-rich and particle-free regions throughout the material.

A monolithic 6061 aluminum alloy was obtained from ALCOA and was used as a control material. This material was produced by ingot metallurgy techniques and was supplied as hot-rolled stock.

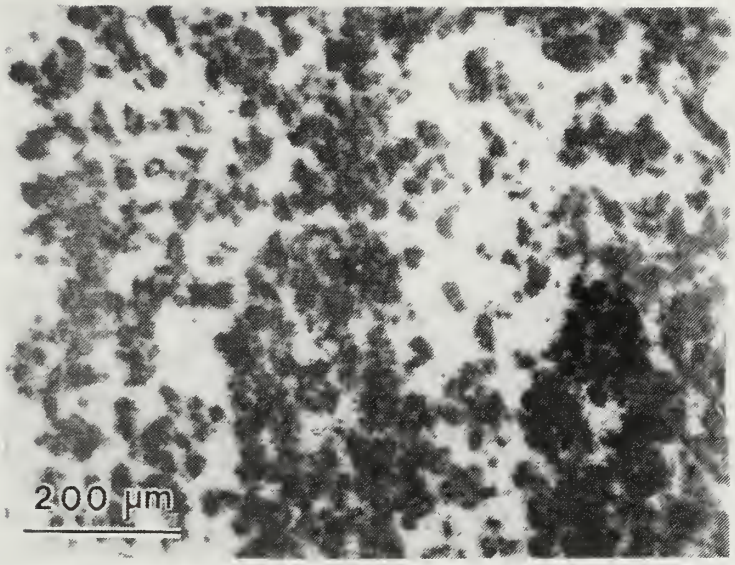


**Figure 2:** Micrograph of the cast and extruded 6061 aluminum - 15 % alumina composite at 100X.

# III. EXPERIMENTAL PROCEDURE

## A. HARDNESS TESTING

The aging characteristics of the 6061 aluminum monolith and the 15% alumina particulate reinforced composite were compared at a temperature of 200° C via microhardness measurements. The composite was cut on a power hacksaw and the 6061 aluminum was cut using a band saw. Ten samples of each material were cut and ground to approximately the same size and to ensure that the top and bottom surfaces of the test specimens was parallel. All pieces were solutionized at 540° C for 90 minutes and quenched in ice water. The aging was done at 200° C with the samples being removed from the oven at various times and quenched in ice water to stop the aging. Each sample was sanded briefly with 600 grit sand paper to clean the surface before hardness readings were taken. The hardness testing equipment used was the Buehler Micromet Vickers Microhardness Tester with a 100 gram load. The load size was chosen to make the indentation small enough to fit between the reinforcement particulates. Care was taken to ensure that the indenter was hitting the matrix material. The length of the two diagonals was measured and several readings were taken for each aging time. These were converted into Vickers Hardness Numbers.

## B. RESISTIVITY

The changes in resistivity accompanying the isothermal aging of both the monolith and the composite were recorded at 20°C, 41°C, 100°C and 200°C. The samples for resistivity measurement were machined to a size of 114.3 mm x 3.8 mm x 1.8 mm.

The rig used for the measurement is shown in Figure 3. More detailed drawings are included in Appendix A. The apparatus consists of four stainless steel probes which rest on the test sample. The two outer probes were connected to a galvanostat which supplied a constant current of 0.5 amperes. The resulting potential between the two inner probes was measured using a digital voltmeter having a sensitivity of 100nV. A computer connected to the voltmeter acquired the voltage data in real-time using a program entitled RESIST.BAS, listed in Appendix B. For these experiments the first hour of data was taken at five second intervals, while for the remainder of the period the data was recorded every five minutes. The measurements were conducted for 24 hours for all samples except the ones aged at 20°C, for which the experiment was conducted for 72 hours. After acquiring elapsed time and voltage, the program converted the voltage to resistance based on the constant current. The time and resistance were recorded in two separate files. An additional program, provided in

Appendix C, combines the two files of time and resistance into one file which was used to graph the results.

The samples were at room temperature before they were

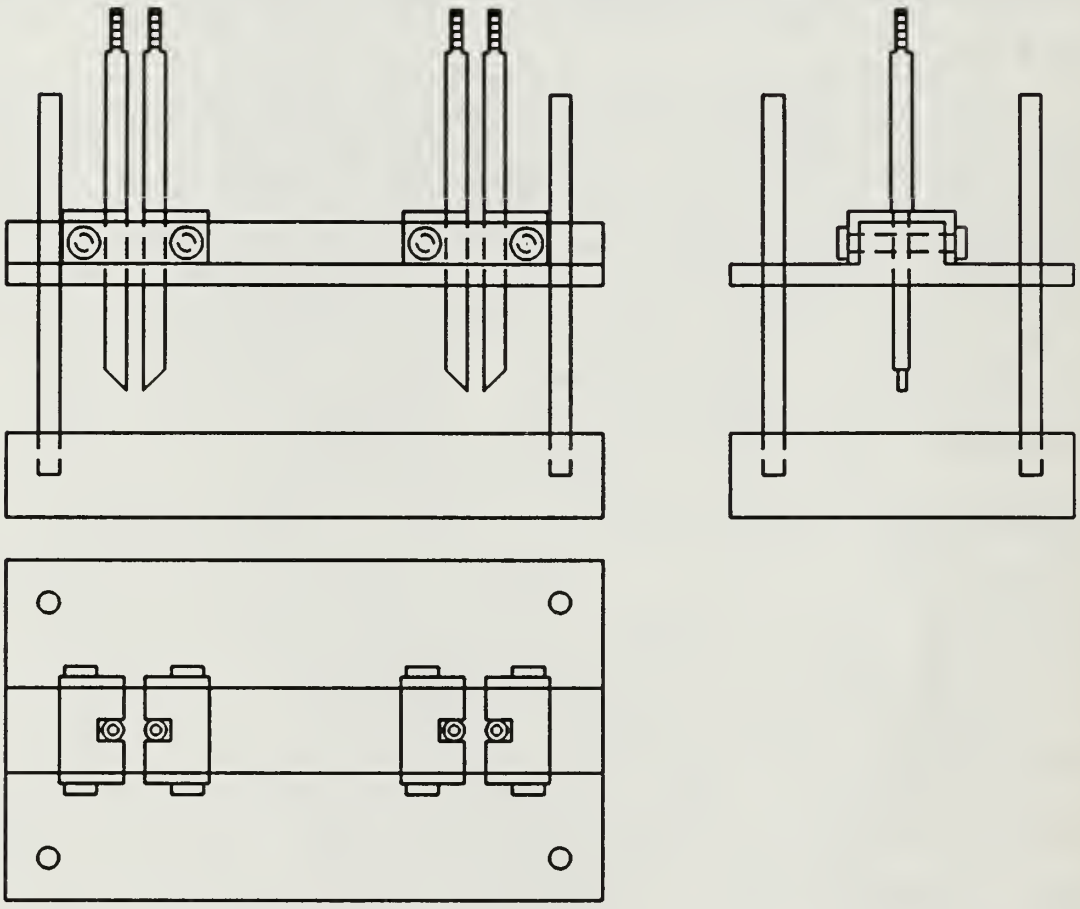

**Figure 3** Apparatus Used to Hold Specimen to Conduct Resistance Measurements, in-situ.

placed in the preheated oven. Based on simple heat transfer calculations, the time for the very thin sample to reach the aging temperature was judged to be negligible. The pieces were solutionized without vacuum sealing based on the results of Osamura and Ogura [Ref. 9], who found no

significant difference between the electrical resistance changes accompanying aging in specimens after solution treatment in a purified argon atmosphere or air. Accordingly, it was suggested that surface oxidation did not affect the essential features of precipitation processes for the specimens.

## C. DIFFERENTIAL SCANNING CALORIMETRY

Heat capacities of the monolithic alloy after different heat treatments were measured as a function of the temperature using the Perkin-Elmer Model Differential Scanning Calorimeter. A 1.5 mm thick strip of 6061 aluminum was sliced on a band saw and disks of 5.5 mm diameter were cut from the strip using electric discharge machining. The specimens were sanded to approximately the same size and then weighed on an analytical balance. Each sample was then sealed in a Vycor tube under vacuum (pressure less than $10^{-4}$ torr) to prevent oxidation during solutionizing. Each sample was solutionized for 90 minutes in a furnace at 540° C, quenched in liquid nitrogen and either aged for 90 minutes at 20° C or placed directly in the DSC.

The lower limit of the DSC, set at 273K, was maintained using a mechanical chiller and the upper limit was set at 813K. A constant heating rate of 10K/minute was used for all the experiments.

For this work a baseline of pure aluminum was not available. Instead the linear formula for the change of specific heat with temperature was utilized. The formula [Ref. 10], in cal/K-mole is:

$$Cp=4.94+2.96x10^{-3}T$$

When converted to the units of kJ/Kg-K for aluminum (atomic weight 26.98 gm/mole) this becomes:

$$C_p=0.766+4.593x10^{-3}T$$

The first exothermic peak of the thermogram, which was tentatively assigned to GP zone formation, was replotted on an enlarged scale for each experiment and the area under the curve was found using a planimeter and checked by graphical integration. The GP zone formation reaction was considered to be first order and the data was reduced using the approach of DeIasi and Adler [Ref. 11].

Assuming the reaction is first order, the rate of reaction is proportional to the concentration of the reacting species:

$$\frac{-dc}{dt}=k_rc$$

where:

$k_r$ = specific reaction rate constant

c = reactant concentration

For the DSC, the rate of heat flow, dH/dt, monitors the rate at which reaction takes place. The concentration of reactant remaining at any time, t, is represented by the total area under the dissolution peak, A, minus the area under the peak to time t, $a_t$. Therefore:

$$\frac{dH}{dt} = k_r(A - a_t)$$

Substituting:

$$dh = \Delta C_p dT$$

and rearranging to solve for the reaction rate yields:

$$k_r = \frac{\Delta C_p dT}{(A - a_t)\, dt}$$

and since a constant heating rate, Q, (in this case 10 K/min) was used:

$$k_r = \frac{Q \Delta C_p}{A - a_t}$$

Using this relationship, values of $k_r$ as a function of

temperature were obtained using stepwise integration of partial areas under the GP zone formation peaks. The value of ln $k_r$ was plotted against temperature and the slope was determined at the respective temperatures to solve for the activation energy, $E_a$, $\Delta H$, activation entropy $\Delta S$ and $\Delta G$ using the following formulae [Ref. 12]:

$$E_a = \frac{RT^2 d(\ln K_r)}{dT}$$

$$\Delta H = E_a - RT$$

$$\Delta S = \frac{\Delta H}{T} + R\ln\left(\frac{hk_r}{kT}\right)$$

$$\Delta G = -RT\ln\left(\frac{hk_r}{kT}\right)$$

The computer program used to perform most of the calculations is documented in Appendix D.

## D. TRANSMISSION ELECTRON MICROSCOPY (TEM)

Samples for TEM examination were prepared from the monolithic 6061 aluminum by slicing approximately 0.25 mm

thick foils on a low speed diamond saw and punching out 3 mm diameter disks from the foils. The samples were then thinned with 600 grit sandpaper to approximately 100 $\mu$m thickness and cleaned in acetone. They were then encapsulated in Vycor tubes under vacuum (pressure less than $10^{-4}$ torr), solutionized for 90 minutes at 540°C and quenched in liquid nitrogen. The specimens were aged in the DSC under the following conditions: 100°C for 100 seconds and 1200 seconds and at 200°C for 3000 seconds and 16 hours (57600 seconds). After the aging treatment the specimens were thinned by twin-jet electropolishing in a Struers Tenupol using a solution of 3% perchloric acid, 62% ethanol, and 35% butoxy-ethanol. The potential was 25V, the temperature was -40 to -50°C and the flow rate was 4.5 to 5.0 on the Tenupol pump control. After thinning, the samples were kept in a freezer (0°C) in an evacuated desiccator until they were examined under the TEM. A JEOL 100CX transmission electron microscope operating at an accelerating voltage of 120 kV was used for all the observations.

## IV. RESULTS AND DISCUSSION

### A. HARDNESS TESTING

A plot of the Vickers Hardness (DPH) of the monolith and the composite matrix, as a function of aging time, at a temperature of 200°C is shown in Figure 4. The following observations can be made from these results.

First, the matrix of the composite materials exhibited a higher microhardness in the solutionized and as-quenched

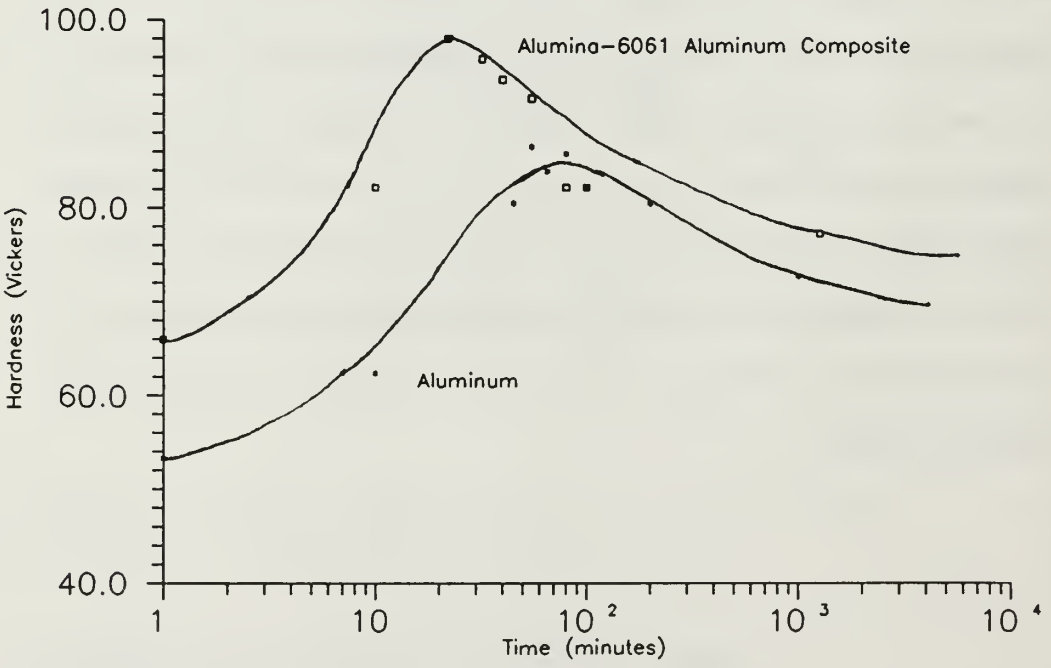


**Figure 4:** Results of Hardness Testing of 15 volume% reinforced $Al_2O_3$ compared to 6061 monolith.

condition than the unreinforced alloy. This same result was obtained with several repetitions of the experiment. Secondly, the peak aging time for the control alloy is about 80 minutes. However, the composite material attained peak hardness in approximately 25 minutes. Given the inherently large scatter in the microhardness measurements, any differences in the peak aging time for the materials cannot be precisely identified. Despite the scatter levels, the aging trends observed in Figure 4 seem to be reproducible in that duplicate measurements in the same aging condition of a composite material exhibited very similar mean values of matrix microhardness.

The microhardness testing of the composite required many iterations because of the large scatter in data. Close to reinforcement particle clusters the hardness was found to be greater than in regions where there are no particles. In addition, the hardness shot up drastically when any of the particles were hit by the indentor. Suresh, Christman and Sugimura [Ref. 5] also recorded large scatter in their microhardness testing.

The initial higher microhardness for the composite was expected based on the theory of increased dislocations in the matrix of the material based on the differences in thermal expansion coefficients of the composite and the matrix material. The linear coefficient of thermal expansion, $\alpha$, for aluminum is $23 \times 10^{-6}/K$ and, therefore, it

contracts more than the alumina which has a linear coefficient of thermal expansion of 7 x $10^{-6}$/K when cooling from the solutionizing temperature. This is expected to deform the matrix plastically around the alumina particles, and also generate residual stress fields in the matrix. Previous work [Ref. 6] based on Al - SiC composites showed similar trends. in $Al_2O_3$, the acceleration of aging is expected to be somewhat less than in Al - SiC because the coefficient of thermal expansion for $Al_2O_3$ is considerably greater than that for SiC, which has a coefficient of thermal expansion of 3 x $10^{-6}$. Consequently, the thermal contraction, stresses and dislocation density are expected to be somewhat less for $Al_2O_3$ composites than those for SiC - Al composites.

## B. EFFECT OF AGING ON RESISTIVITY AND MICROSTRUCTURE

The results of the in-situ resistivity measurements are shown in Figures 5 - 8. These plots compare the monolith and the composite material. Figure 5 indicates that the resistivity changes accompanying aging can be broadly divided into three zones which define the changes in the microstructure.

Zone I is associated with the rapid rise of resistivity. This is associated with the growth of vacancy clusters, dislocation loops and probably some silicon atom clustering. This is confirmed by the TEM micrographs in Figures 9A and

B, which show the microstructure of a monolithic 6061 aluminum sample aged at 373K for 100 seconds. These figures show a high density of small dislocation loops in the matrix. Some of the loops seem to have small precipitates (probably silicon clusters) associated with them.

The second zone is the region over which the resistivity remains fairly constant with time. The microstructural changes accompanying the initial part of Zone II are seen in Figures 10A and B. This sample was aged at 373K for 1200 seconds and the matrix is seen to be densely populated by very small precipitate clusters, tentatively identified as silicon clusters. Silicon clustering is known to be the first step in the precipitation process in aluminum-magnesium-silicon alloys. [Ref. 2] The latter part of Zone II is characterized by Figures 11A and B which show the bright and dark fields of a TEM micrograph of a 6061 aluminum sample aged at 473K for 3000 seconds. The transmission electron micrograph shows very small needle-shaped precipitates, approximately 10-30 nm long, situated along <100> directions of the aluminum lattice. The streaking along the <110> and <012> directions of the selected area diffraction pattern (zone axis is [112]) indicates that the precipitates produce strong strain fields along these directions suggesting that the needles are at least partially coherent. Some thicker and longer needles and even some rods are also visible. It is therefore

concluded that the latter part of Zone II of the resistivity vs. time curves is associated with the growth of GP zones and transition $\beta$.

Plate shaped precipitates on the {100} planes of the aluminum are seen to be present in the bright-field and dark-field TEM micrographs of the sample aged for 16 hours at 473K (Figures 12A and B). This is indicated by the <100> streaking in the $\vec{z}$ = [001] selected area diffraction pattern (SADP). Some of the precipitates which are on the (001) faces of the aluminum lattice are seen to be leached out during polishing. These plates are the equilibrium $\beta$ - $Mg_2Si$ precipitates. Zone III is therefore associated with the growth of $\beta$ - $Mg_2Si$.

## C. COMPARISON OF RESISTIVITY CHANGES IN MONOLITH AND COMPOSITE

It can be seen from Figure 5 that during aging at 473K, Zone I for the composite is shorter than for the monolith. Zone II begins and ends earlier, and Zone III is also accelerated. The acceleration of silicon clustering (Zone I) in the composite is more evident in the isothermal resistivity curve at 373K (Figure 6) where the Zone I is seen to be considerably shortened compared to that of the monolith. Figure 7, which plots the change of resistivity during isothermal aging at 324 K also depicts the shortened Zone I of the composite in comparison with the monolith.

The resistivity change with natural (room temperature) aging (Figure 8) is at variance with the resistivity plots at other aging temperatures. It indicates that the composite resistivity remains relatively constant while that of the monolith increases. The results were duplicated and are not yet fully understood. One explanation might be that at 293K the quenched in vacancies diffuse to the matrix dislocations in the composite instead of coalescing and growing, thereby keeping the resistivity fairly constant with time. In the monolith, however, there are few dislocations to which the quenched in vacancies can diffuse and hence the dislocation loops grow with aging.

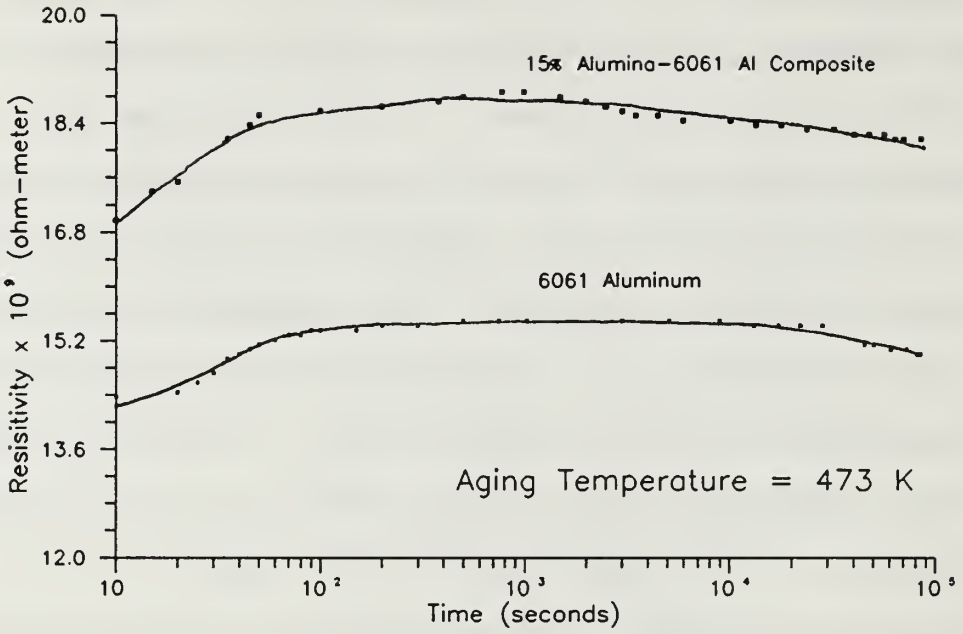


**Figure 5** Resistivity of Alumina-6061 Aluminum Composite and 6061 Aluminum as a Function of Time at 473K.

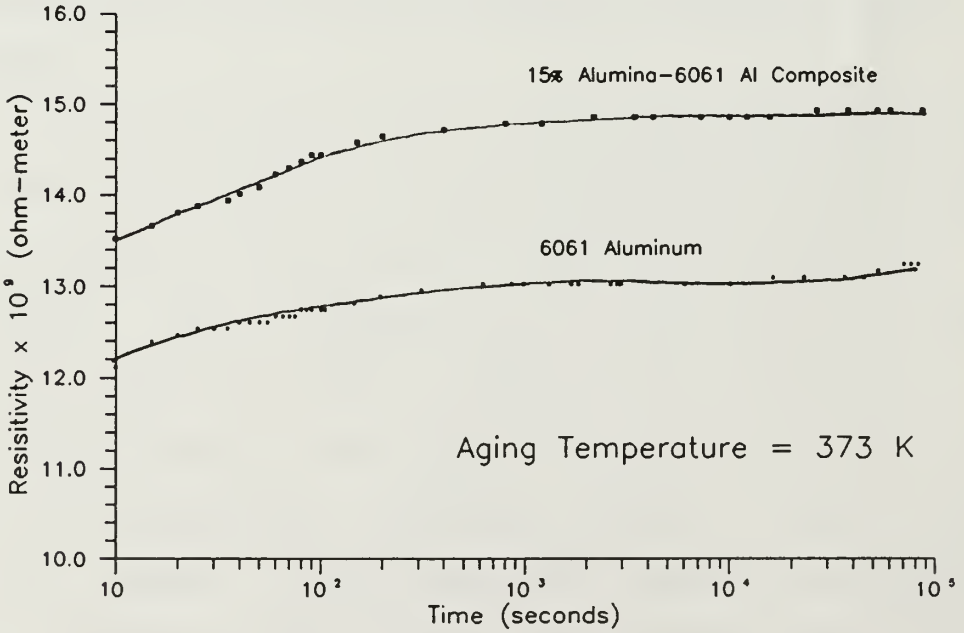


**Figure 6** Resistivity of Alumina-6061 Aluminum Composite and 6061 Aluminum as a Function of Time at 373K.

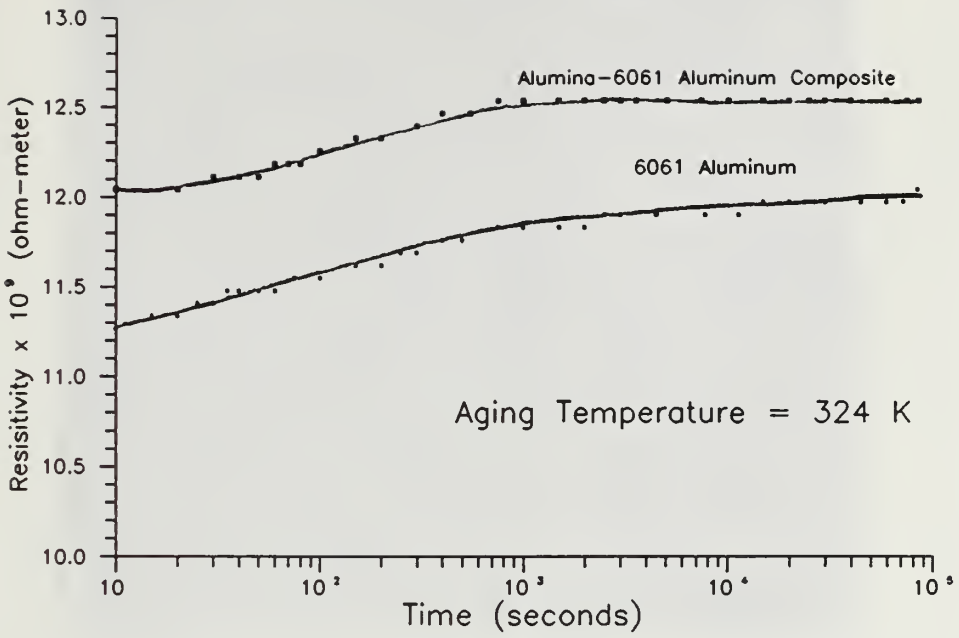


**Figure 7** Resistivity of Alumina-6061 Aluminum and 6061 Aluminum as a Function of Time at 324K.

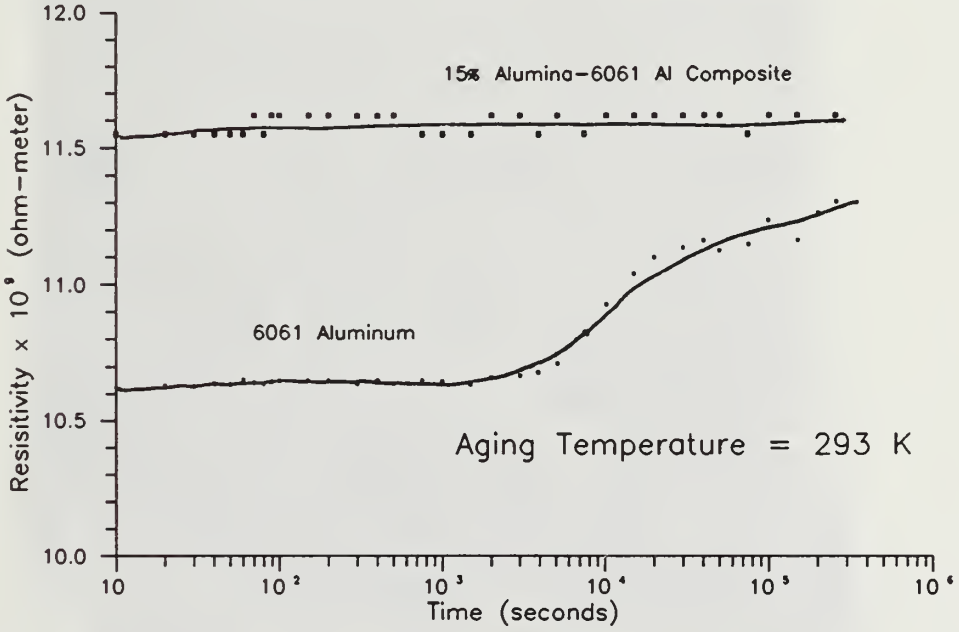


**Figure 8** Resistivity of Alumina-6061 Aluminum Composite and 6061 Aluminum as a Function of Time at Room Temperature.

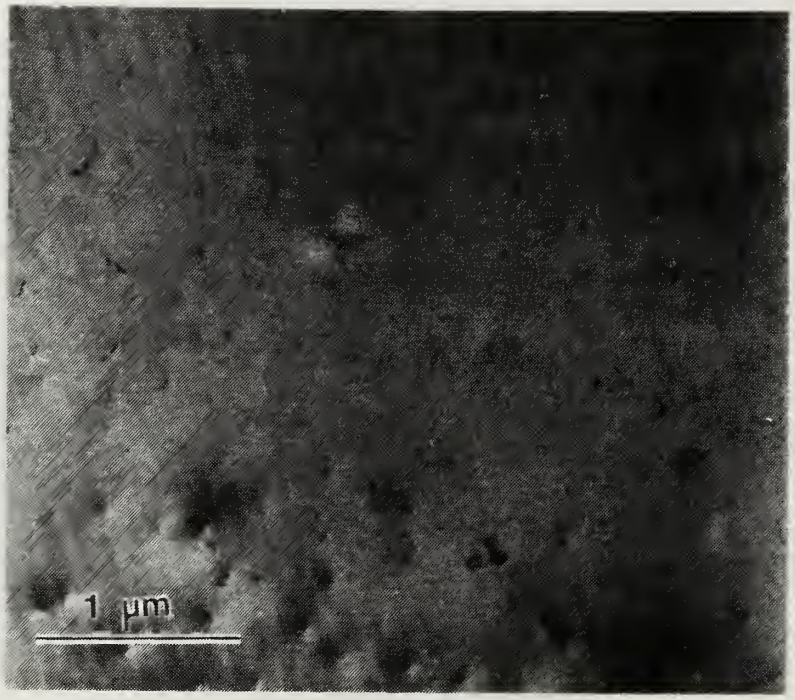


**Figure 9A** Bright-field TEM Micrograph of 6061 Aluminum Aged for 100 Seconds at 373K.

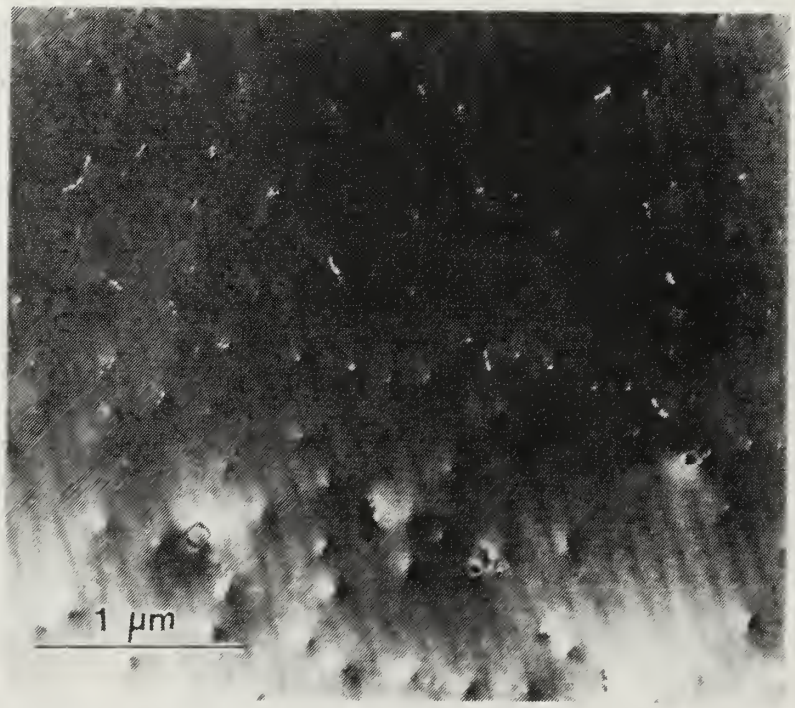


**Figure 9B** Dark-field TEM Micrograph of 6061 Aluminum Aged for 100 Seconds at 373K.

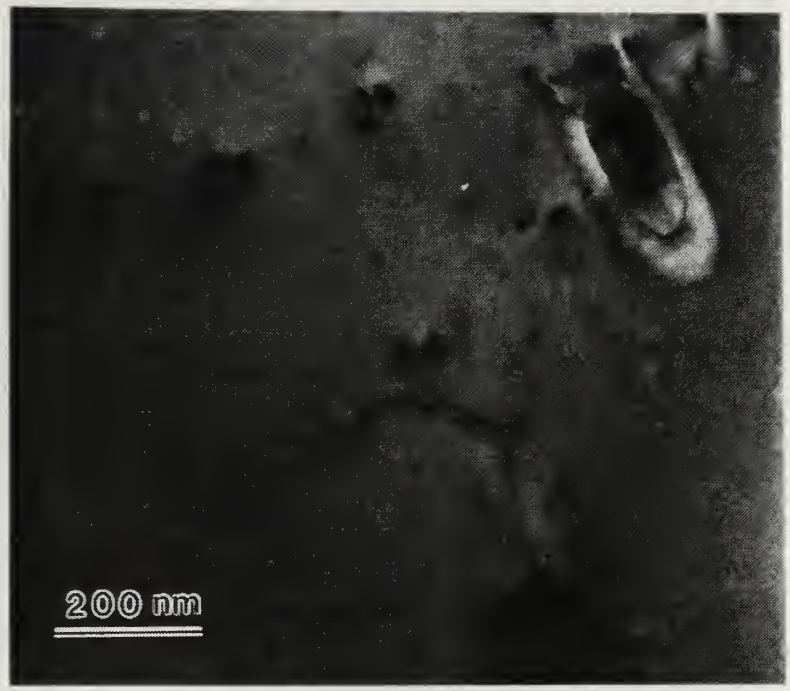


**Figure 10A** Bright-field TEM Micrograph of 6061 Aluminum Aged for 1200 Seconds at 373K.


**Figure 10B** Dark-field TEM Micrograph of 6061 Aluminum Aged for 1200 Seconds at 373K.

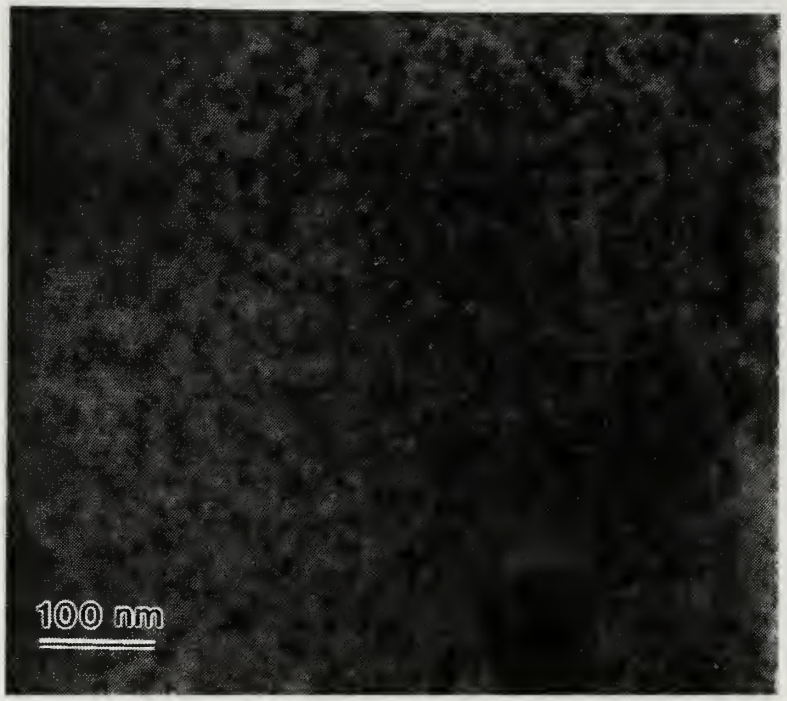


**Figure 11A** Bright-field TEM Micrograph of 6061 Aluminum Aged for 3000 Seconds at 473K.

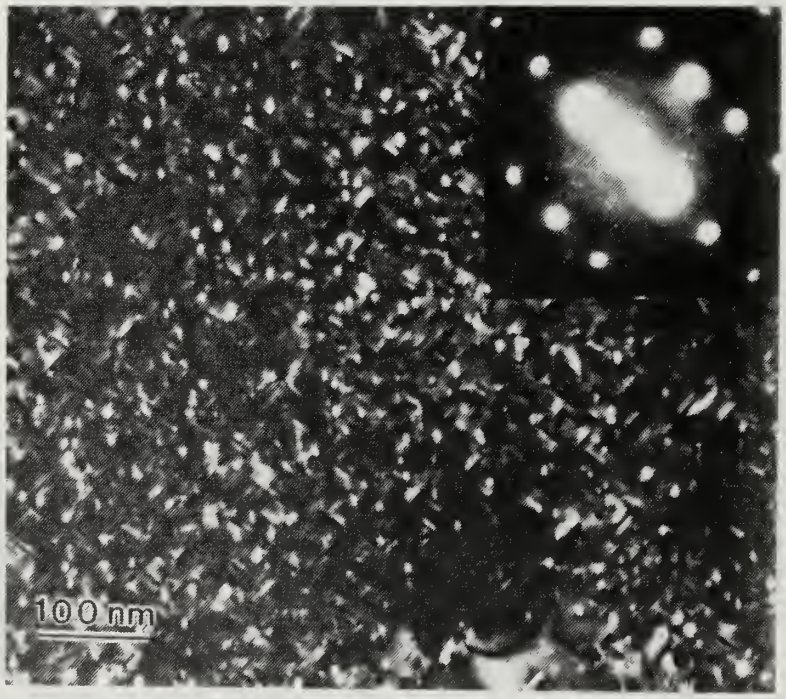


**Figure 11B** Dark-field TEM Micrograph of 6061 Aluminum Aged for 3000 Seconds at 473K.


**Figure 12A** Bright-field TEM Micrograph of 6061 Aluminum Aged for 16 Hours at 473K.


**Figure 12B** Dark-field TEM Micrograph of 6061 Aluminum Aged for 16 Hours at 473K.

## D. DIFFERENTIAL SCANNING CALORIMETRY

The precipitation kinetics of the monolith 6061 aluminum were monitored with the DSC. A typical DSC thermogram with the various peaks labeled is shown in Figure 13. The first exothermic peak is due to GP zone formation, the second

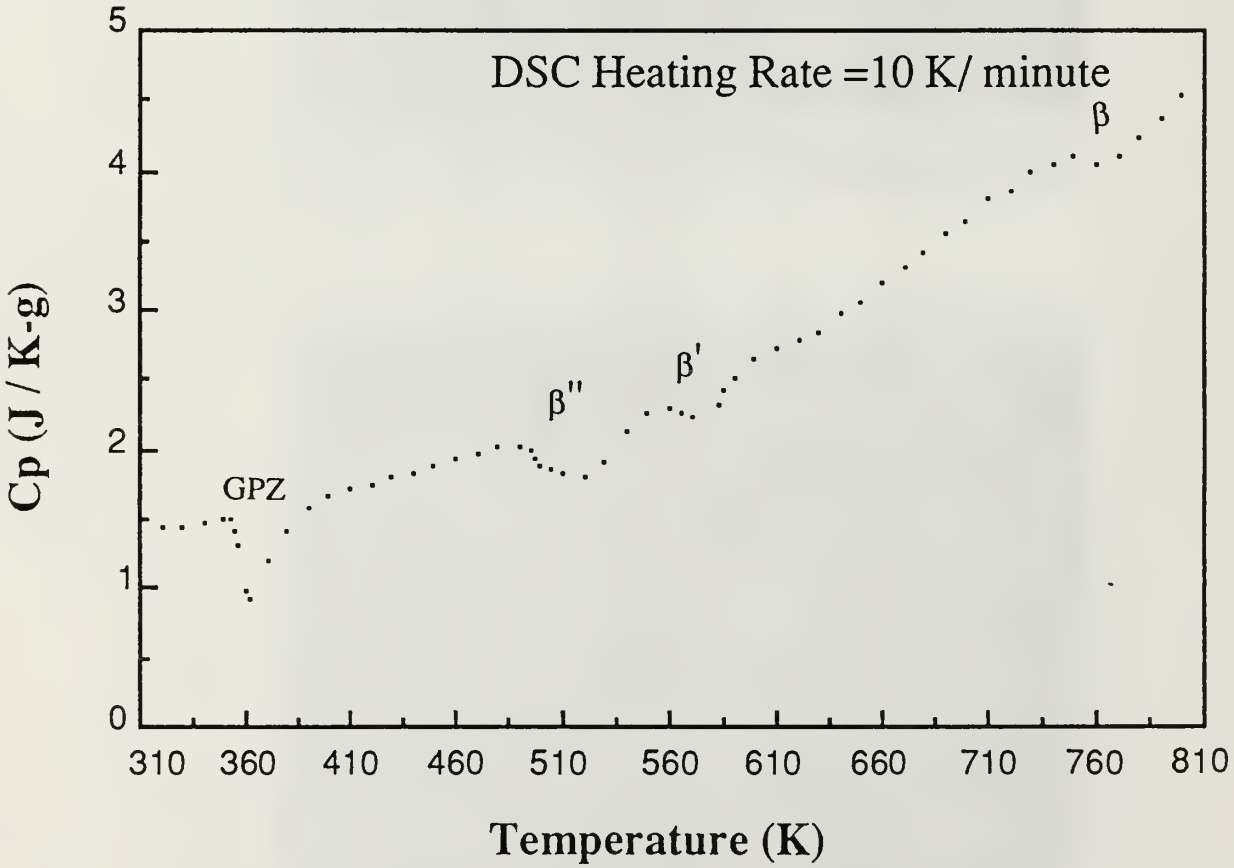


**Figure 13** A representative DSC thermogram of a monolithic 6061 aluminum. The curve above was obtained by scanning a sample which was solutionized and quenched and aged for 5400 seconds at room temperature.

exotherm is for $\beta''$ formation, the third exotherm is for $\beta'$ formation and the final exotherm is for equilibrium $\beta$ formation. An exotherm corresponding to $\beta$ dissolution exists above 810K. The intermediate $\beta''$ and $\beta'$ peaks seem to be partially superimposed on one another. The general nature of the precipitation sequence in the DSC thermogram remained unaltered due to the various heat treatments used in this study.

The kinetic study was concentrated on the early stages of precipitation, i.e., GP zone formation. The results are presented in Table I.

**TABLE I: PRELIMINARY DSC RESULTS**

| | $T_p$ | $H_R$ | $E_a$ | $\Delta G^*$ | $\Delta H^*$ | $\Delta S^*$ |
|---|---|---|---|---|---|---|
| | K | kJ/kg | kJ/mole | kJ/kg | kJ/kg | kJ/kg-K |
| 6061 No Aging | 418 | 34.3 | 63.30 ±30.13 | 4515.80 ±56.70 | 2212.27 ±1118.9 | -5.2619 ±2.5367 |
| 6061 RT Age | 362 | 19.0 | 55.98 ±18.63 | 3958.53 ±84.14 | 1956.78 ±696.3 | -5.1626 ±1.8830 |

Aging the material dropped the GP zone formation peak temperature, $T_p$, from 418K to 362K. Correspondingly, the heats of reaction also dropped since a smaller volume fraction of the GP zones formed during the DSC scan and the

heat of reaction is proportional to the volume fraction of the precipitates. The activation energy ($E_a$) and the activation free energy ($\Delta G^*$) also dropped, indicating that pre-existing precipitation sites preclude the formation of new nuclei, thereby reducing the activation barrier to precipitation. In general, the activation enthalpy ($\Delta H^*$) showed trends similar to that of $\Delta G^*$. On the other hand the activation entropy ($\Delta S^*$) changed very little. It can therefore be concluded that the enthalpy change and not the entropy change is the principal factor determining the activation barrier to GP zone formation.

The objective of the DSC studies on the monolithic 6061 Al was to establish the background for comparison to precipitation in the composite, which will be done as a continuation of this work.

## V. CONCLUSIONS

Reinforcement of cast 6061 Aluminum with $Al_2O_3$ particles results in appreciable acceleration of aging. The hardness testing results show that for an aging temperature of 200°C, the alumina-6061 aluminum composite reaches peak hardness in approximately 30 minutes as opposed to the 80 minutes required for the monolithic 6061 Aluminum control sample.

Resistivity measurements coupled with TEM observations reveal that Si clustering at vacancy loops initiates earlier in the Alumina-6061 Aluminum composite. Growth of plate shaped $\beta$-$Mg_2Si$, indicated by the final drop in resistivity, starts earlier in the alumina-6061 aluminum composite than in the monolith. The early clustering of Si atoms at vacancy loops, and the early growth of $\beta$-$Mg_2Si$ plates indicate that the overall aging of the alumina-6061 aluminum composite is accelerated.

Preliminary DSC studies of the early stages of precipitation in 6061 aluminum suggest that this technique is a good tool to evaluate the thermodynamic and kinetic effects of reinforcement on GP zone formation in the alumina-6061 aluminum composite matrix.

## VI. RECOMMENDATIONS

The resistivity measurement apparatus was originally designed along ASTM B 63 - 49 for four wire resistance measurements. A sufficiently sensitive ohmmeter was not available to measure the resistivity of the samples, so the apparatus was modified to read the potential drop across the two inner probes while a constant current was passed through the specimen from the outer two probes. Difficulties were encountered maintaining good contact between the probes and the specimens, especially at elevated temperatures. A new apparatus was designed and is shown in Figure 14. Detailed drawings are included in Appendix A.

In the new apparatus the probes are fixed to the top block, the wires to the DMM are secured in a hole by a set screw and current is supplied to the piece from a constant current power supply alligator clips. This should alleviate the problems encountered with the probes shifting and losing contact as in the original design.

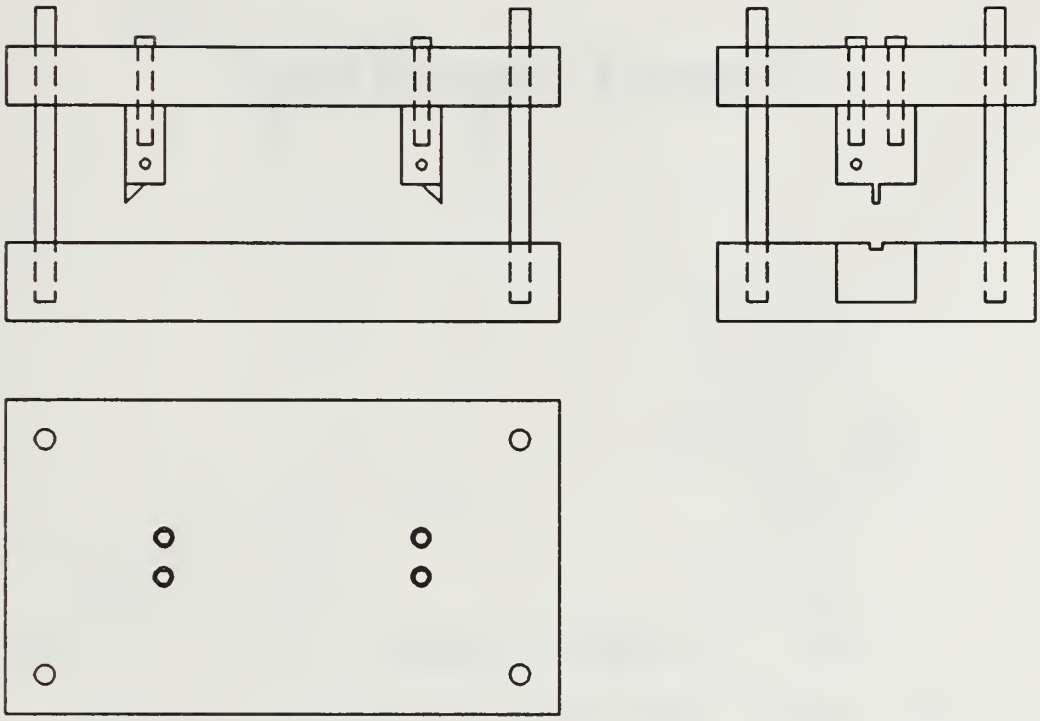

**Figure 14** New Resistivity Test Rig for in-situ Measurements.

## APPENDIX A: APPARATUS DESIGN

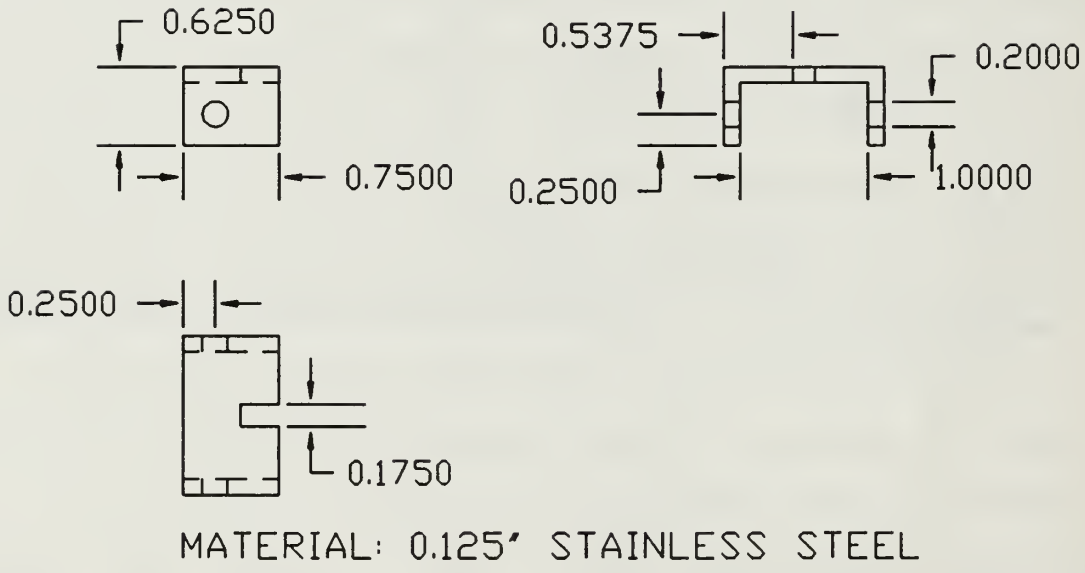


**Figure A1** Guide to position probes on current test rig. Four required.

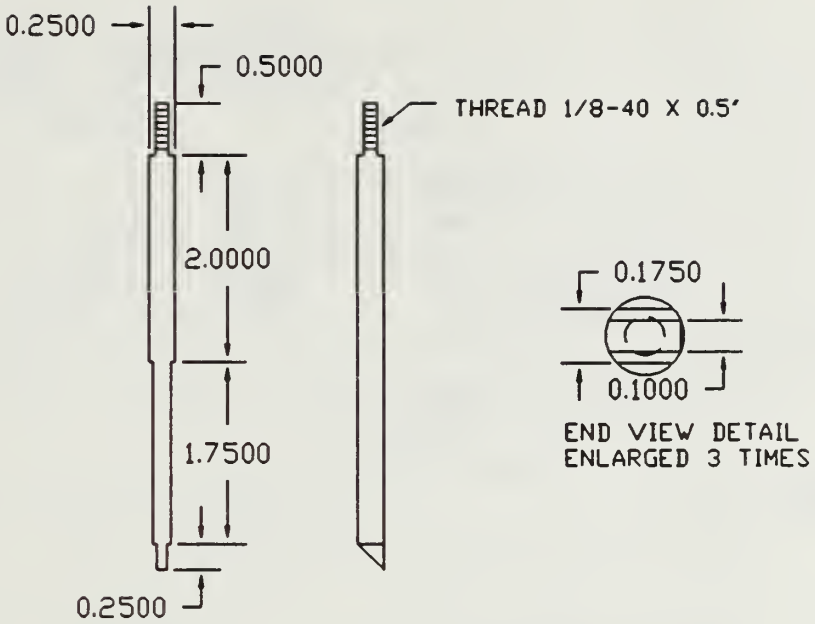


**Figure A2** Probes for applying current and reading voltage. Four required.

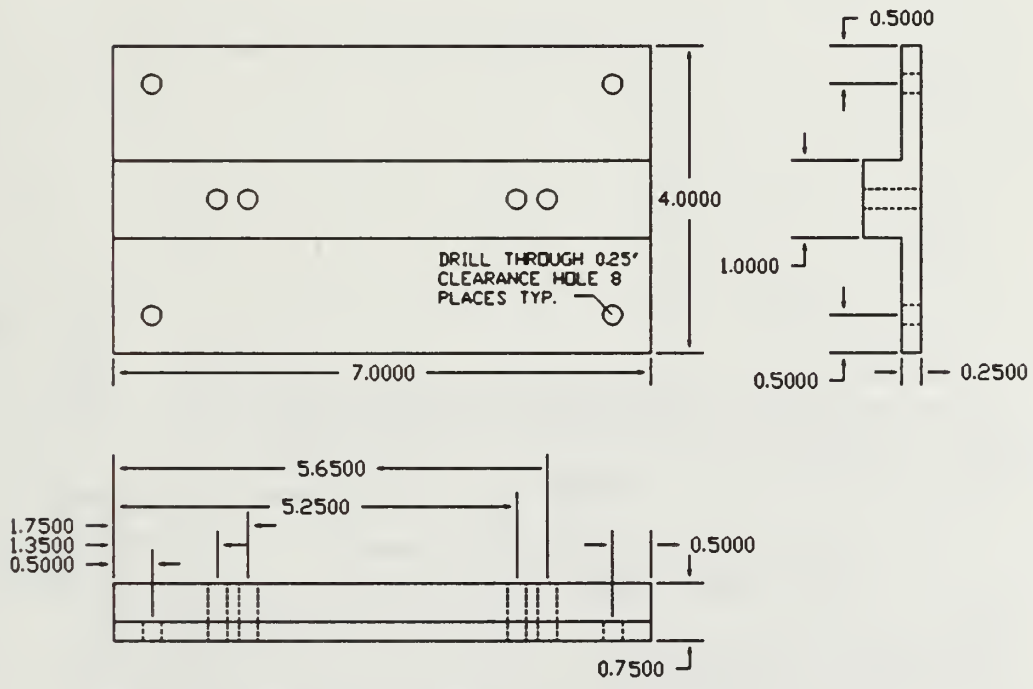


**Figure A3** Top of present test rig. One required.

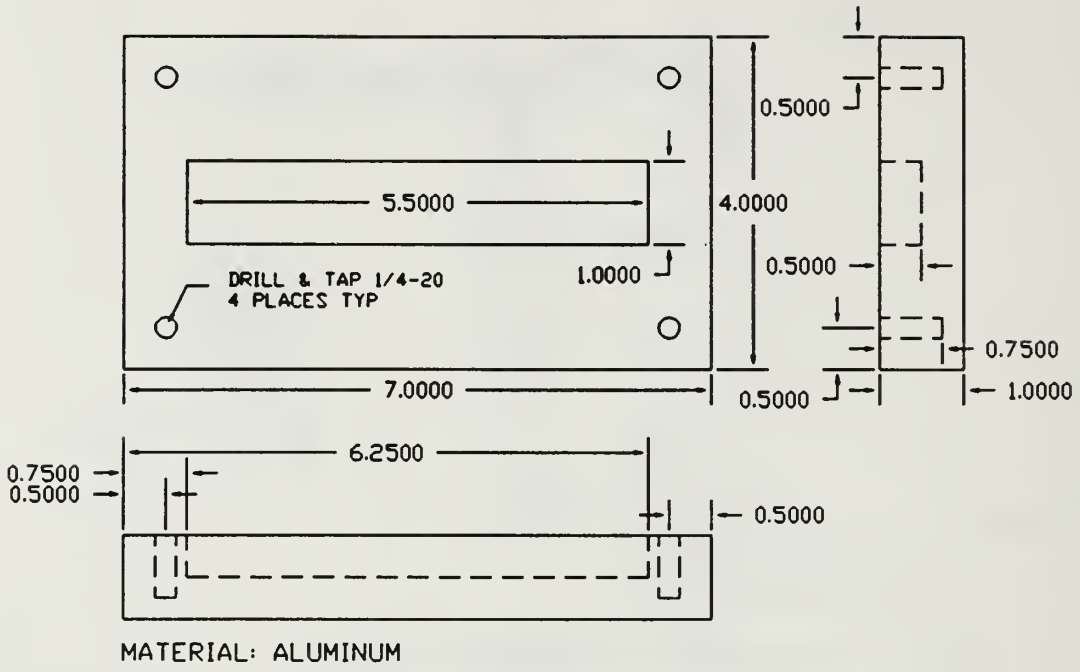


**Figure A4** Base of present test rig. One required.

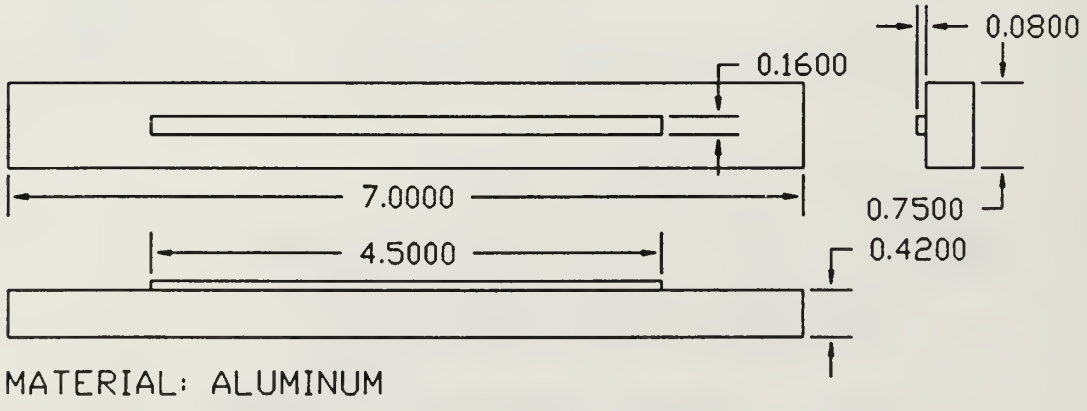


**Figure A5** Pattern for molding castable ceramic to hold specimen. One required.

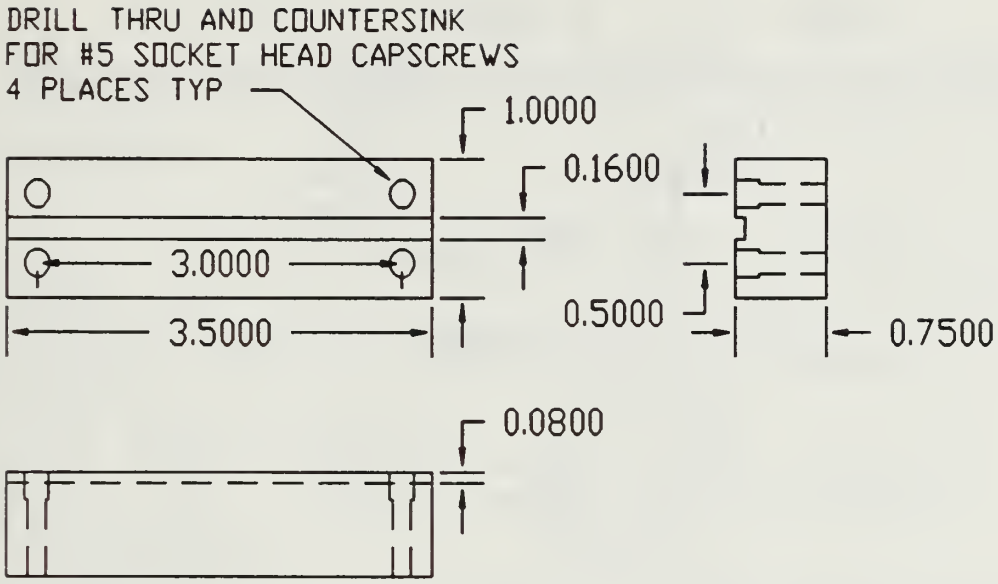


**Figure A6** Block to position specimen in new test rig. One required.

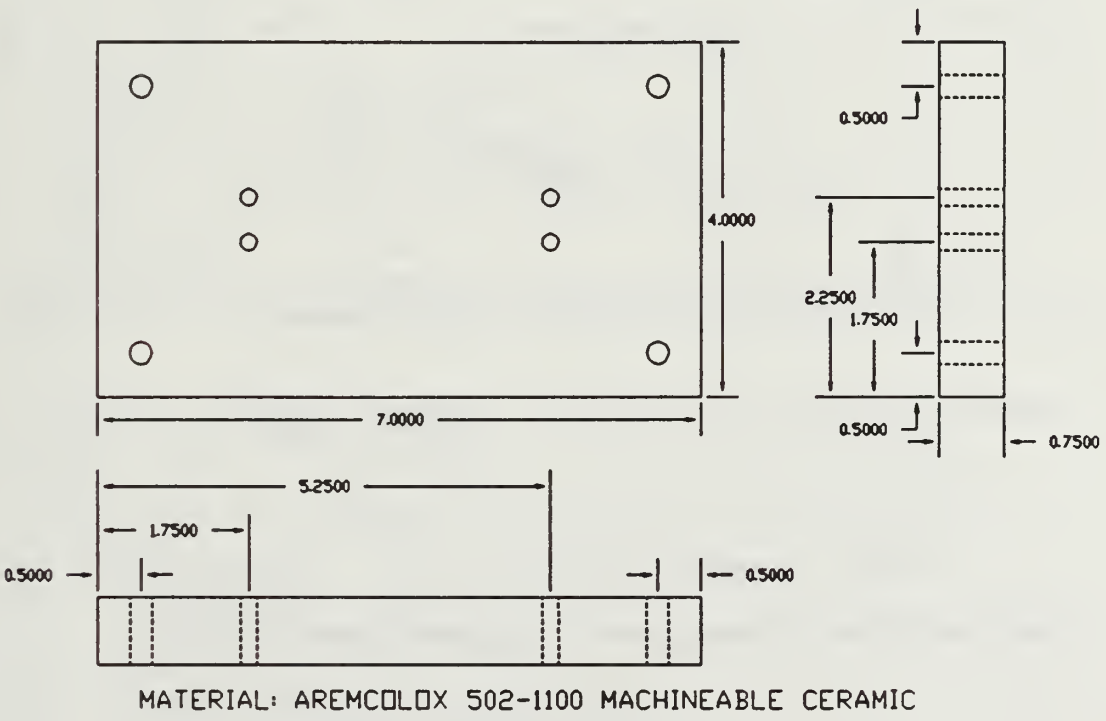


**Figure A7** Top of new test rig. One required.

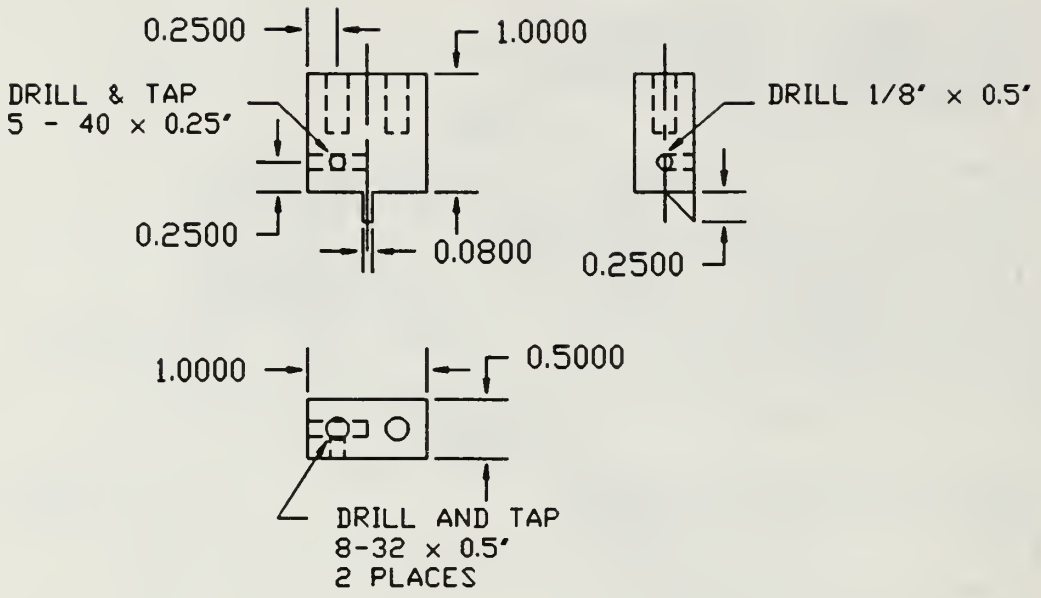


**Figure A8** Probe for new test rig. Two required.

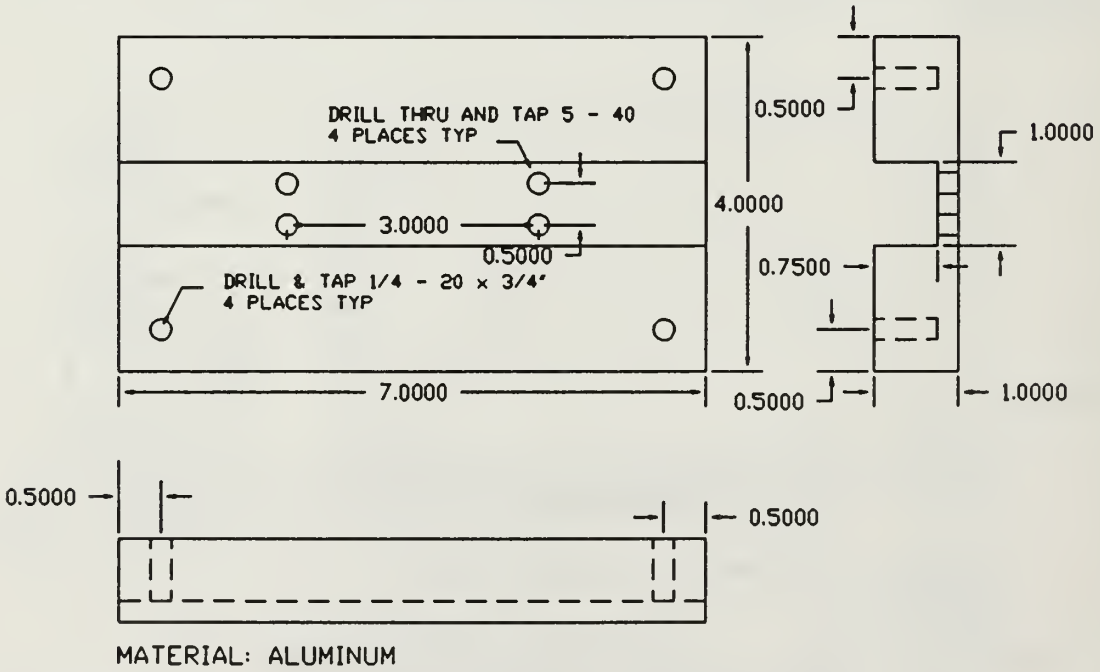


**Figure A9** Base of new test rig. One required.

## APPENDIX B: COMPUTER PROGRAM TO PERFORM RESISTANCE MEASUREMENT

```
10 REM   RESIST.BAS -- PROGRAM TO READ MILLIVOLTS FROM
HP3478A
20 REM  AND CALCULATE RESISTANCE FROM E=IR
30  REM WRITTEN BY R. HAFLEY. LAST MODIFIED 10/5/89 BY R.
HAFLEY
40 REM  DECLARE VARIABLES
50 MAXX = 640   'NUMBER OF PIXELS IN THE X DIRECTION
60 MAXY = 350   'NUMBER OF LINES IN THE Y DIRECTION
70 DIM READNO(6)
80 READNO(0)=0
90 INTERVAL! = 0         'TIME IN SECONDS BETWEEN READINGS
100 DIM INTERVALS(6)
110 INTERVALS(0)=0
120 OHMSRANGE# = 0        'MAX RESISTANCE EXPECTED
130 CMD1$ = ""   'GPIB COMMAND STRINGS
140 CURRENT! = 0          'IMPRESSED CURRENT
150 RESISTFILE$ = ""      'DATA FILE TO STORE RESISTANCE
VALUES
160 TIMEFILE$ = ""        'DATA FILE TO STORE TIME VALUES
500 GOSUB 1000
510 GOSUB 2000  'DRAW GRAPH
520 GOSUB 2500  'INIT GPIB
530 GOSUB 3000  'TAKE READINGS
540 GOSUB 4000  'CLOSE DOWN FILES, ETC.
550 END
1000 KEY OFF
1010 SCREEN 9   'HI RES EGA MODE 640 X 350 16 COLOR
1020 COLOR 7,1  'FOREGROUND = WHITE (7), BACKGROUND = BLUE
(1)
1030 CLS
1040 INPUT "SPECIFY NUMBER OF DIFFERENT INTERVALS FOR
READINGS (MAX = 5)";INTNUM
1050 CLS
1060 FOR I=1 TO INTNUM
1070 ANSWER$ = "N"
1080 WHILE ANSWER$ = "N" OR ANSWER$ = "n"
1090    READNO(I) = 1000
1100    PRINT "DEFAULT NUMBER OF READINGS IS",READNO(I)
1110    A% = 0
1120    INPUT "NUMBER OF READINGS";A%
1130    IF A%<>0 THEN READNO(I)=A%
1140    PRINT "YOU HAVE SPECIFIED"READNO(I)"READINGS."
```

```
1150    INPUT "IS THIS CORRECT (Y/N)";ANSWER$
1160    CLS
1170 WEND
1180 ANSWER$ = "N"
1190 WHILE ANSWER$ = "N" OR ANSWER$ = "n"
1200    INTERVALS(I)=10
1210    PRINT "DEFAULT INTERVAL IS"INTERVALS(I)"SECONDS."
1220    A=0
1230    INPUT "TIME IN SECONDS BETWEEN READINGS";A
1240    IF A<>0 THEN INTERVALS(I)=A
1250    PRINT "YOU HAVE SPECIFIED A"INTERVALS(I)"SECOND
INTERVAL BETWEEN READINGS."
1260    INPUT "IS THIS CORRECT (Y/N)";ANSWER$
1270    CLS
1280 WEND
1290 NEXT I
1300 ANSWER$ = "N"
1310 WHILE ANSWER$ = "N" OR ANSWER$ = "n"
1320    INPUT "MAXIMUM RESISTANCE EXPECTED";OHMSRANGE#
1330    PRINT "YOU HAVE SPECIFIED"OHMSRANGE#"OHMS."
1340    INPUT "IS THIS CORRECT (Y/N)";ANSWER$
1350    CLS
1360 WEND
1370 ANSWER$ = "N"
1380 WHILE ANSWER$ = "N" OR ANSWER$ = "n"
1390    CMD1$="F1R-2N5T1"
1400    PRINT "HP 3478A IS IN 30mV DC RANGE BY CMD
'F1R-2N5T1'."
1410    A$=""
1420    INPUT "STRING TO PUT HP 3478A IN CORRECT MODE";A$
1430    IF A$<>"" THEN CMD1$=A$
1440    PRINT "YOU HAVE ENTERED "CMD1$"."
1450    INPUT "IS THIS CORRECT (Y/N)";ANSWER$
1460    CLS
1470 WEND
1480 ANSWER$ = "N"
1490 WHILE ANSWER$ = "N" OR ANSWER$ = "n"
1500    INPUT "IMPRESSED CURRENT FROM GALVANOSTAT";CURRENT!
1510    PRINT "YOU HAVE SPECIFIED"CURRENT!"AMPS."
1520    INPUT "IS THIS CORRECT (Y/N)";ANSWER$
1530    CLS
1540 WEND
1550 ANSWER$ = "N"
1560 WHILE ANSWER$ = "N" OR ANSWER$ = "n"
1570    PRINT "YOU NEED TO SPECIFY THE NAMES OF THE DATA
FILES THAT YOU WANT."
1580    PRINT "DATA WILL BE STORED IN ASCII FORM."
1590    PRINT "FILENAMES CAN BE UP TO 8 CHARACTERS LONG, AN
EXTENSION OF .DAT"
1600    PRINT "WILL AUTOMATICALLY BE PROVIDED."
1610    INPUT "RESISTANCE DATA FILE";RESISTFILE$
```

```
1620    INPUT "TIME DATA FILE";TIMEFILE$
1630    PRINT "RESISTANCE DATA WILL BE STORED IN FILE
'"RESISTFILE$".DAT'."
1640    PRINT "TIME DATA WILL BE STORED IN FILE
'"TIMEFILE$".DAT'."
1650    INPUT "IS THIS CORRECT";ANSWER$
1660    CLS
1670 WEND
1680 OPEN RESISTFILE$+".DAT" FOR OUTPUT AS #1
1690 OPEN TIMEFILE$+".DAT" FOR OUTPUT AS #2
1700 RETURN
2000 XINT = CINT(MAXX/12)       'BREAK SCREEN INTO 12
PORTIONS
2010 YINT = CINT(MAXY/12)       'DITTO
2020 FOR I = 1 TO 11
2030    LINE (I*XINT-1, YINT-1)-(I*XINT-1, 11*YINT-1)  'VERT
LINES
2040    LINE (XINT-1, I*YINT-1)-(11*XINT-1, I*YINT-1)
'HORIZ LINES
2050 NEXT I
2060 DURATION = 0
2070 FOR I=1 TO INTNUM
2080    DURATION = READNO(I) * INTERVALS(I) + DURATION
2090 NEXT I
2100 RETURN
2500 DEF SEG = &HD000   'BASE ADDRESS OF IEE488 BOARD
2510 BRD% = 0   'DEFINE IEEE488 BOARD
2520 CMD2$ = "SYSCON MAD=3, CIC=1, NOB=1, BA0=&H300"  'INIT
BOARD
2530 CMD3$ = "CONFIG MTA,LISTEN=23"   'SET DMM AS LISTENER
2540 CMD4$ = "CLEAR 23"       'CLEAR DMM
2550 CMD5$ = "OUTPUT 23[$]             'SEND COMMAND STRING
2560 IE488 = 0
2570 CALL IE488 (CMD2$, A%, FLAG%, BRD%)      'INIT BOARD
2580 IF FLAG% <> 0 THEN PRINT "INSTALLATION ERROR":END
2590 CALL IE488 (CMD3$, A%, FLAG%, BRD%)
2600 IF FLAG% <> 0 THEN PRINT "ERROR "HEX$(FLAG%)"IN LINE
2590":END
2610 CALL IE488 (CMD4$, A%, FLAG%, BRD%)
2620 IF FLAG% <> 0 THEN PRINT "ERROR "HEX$(FLAG%)"IN LINE
2610":END
2630 CALL IE488 (CMD5$, CMD1$, FLAG%, BRD%)
2640 IF FLAG% <> 0 THEN PRINT "ERROR "HEX$(FLAG%)"IN LINE
2630":END
2650 RETURN
3000 MV#=0!     'STORAGE FOR MILLIVOLT READINGS
3010 STARTTIME#=0!       'STORE START TIME
3020 OHMS#=0!   'CALCULATED OHMS
3030 TIME#=0!   'READING TIME
3040 READING$="               "     'INIT READING STRING
3050 CMD6$ = "ENTER 23[$,0,18]"
```

```
3060 PRINT "PRESS ENTER TO START DATA ACQUISITION."
3070 A$ = ""
3080 WHILE A$=""  'LOOP TILL KEY STRUCK
3090 A$ = INKEY$
3100 WEND
3110 STARTTIME#=TIMER    'GET START TIME OF TEST
3120 CALL IE488 (CMD6$,READING$,FLAG%,BRD%)     'GET READING
3130 TIME#=TIMER         'GET TIME OF READING
3140 IF FLAG% <> 0 THEN PRINT "ERROR "HEX$(FLAG%)" IN LINE
3120."
3150 B$=MID$(READING$,2,7)      'STRIP GARBAGE FROM STRING
3160 MV#=VAL(B$)         'CONVERT STRING TO DOUBLE PRECISION
3170 OHMS#=MV#/(1000!*CURRENT!)    'CALCULATE RESISTANCE
3180 TESTTIME# = TIME#-STARTTIME#        'CALCULATE ELAPSED
TIME
3190 WRITE#1,OHMS#     'WRITE OHMS TO FILE
3200 WRITE#2,TESTTIME# 'DITTO WITH TIME
3210 X = 10 * TESTTIME# * XINT / DURATION + XINT 'CALC WHERE
TO PLOT X
3220 Y = (YINT * 11) - 10 * YINT * OHMS# / OHMSRANGE#
'DITTO FOR Y
3230 PSET(X,Y),14         'PLOT POINT
3240 FOR J = 1 TO INTNUM
3250 INTERVAL!=INTERVAL!+READNO(J-1)*INTERVALS(J-1)
3260 FOR I = 1 TO READNO(J)
3270 WHILE
(TIME#-STARTTIME#)<(I*INTERVALS(J)+INTERVAL!)'READY FOR NEXT
READING?
3280    TIME#=TIMER     'GET NEW TIME
3290 WEND       'END LOOP
3300 CALL IE488 (CMD6$,READING$,FLAG%,BRD%)     'GET READING
3310 TIME#=TIMER         'GET TIME OF READING
3320 IF FLAG% <> 0 THEN PRINT "ERROR "HEX$(FLAG%)" IN LINE
1645."
3330 B$=MID$(READING$,2,7)      'STRIP GARBAGE FROM STRING
3340 MV#=VAL(B$)         'CONVERT STRING TO DOUBLE
PRECICISION
3350 OHMS# = CURRENT! * MV# / 1000!     'CALCULATE
RESISTANCE
3360 TESTTIME# = TIME# - STARTTIME#     'CALCULATE ELAPSED
TIME
3370 WRITE#1,OHMS#       'WRITE OHMS TO FILE
3380 WRITE#2,TESTTIME#  'DITTO WITH TIME
3390 X = 10 * TESTTIME# * XINT / DURATION + XINT 'CALC WHERE
TO PLOT X
3400 Y = (YINT * 11) - 10 * YINT * OHMS# / OHMSRANGE#
'DITTO FOR Y
3410 PSET(X,Y),14         'PLOT POINT
3420 NEXT I
3430 NEXT J
3440 RETURN
```

```
4000 CLOSE       'CLOSE DATA FILES 1 & 2
4010 LOCATE 1,1
4020 PRINT "                                                    "
4030 LOCATE 1,1
4040 PRINT "TEST COMPLETED";CHR$(7)
4050 RETURN
```

## APPENDIX C. PROGRAM TO COMBINE RESISTANCE AND TIME FILES

```
10 REM PROGRAM TO COMBINE SEVERAL ASCII DATA FILES FOR
GRAPHER
20 REM WRITTEN 10-6-89 BY R. HAFLEY
30 INPUT"WHAT'S THE FIRST FILE NAME";FIRSTFILENAME$
40 INPUT "WHAT'S THE SECOND FILE NAME";SECONDFILENAME$
50 INPUT "WHAT FILE TO WRITE TO";WRITEFILE$
60 OPEN FIRSTFILENAME$ FOR INPUT AS #1
70 OPEN SECONDFILENAME# FOR INPUT AS #2
80 OPEN WRITEFILE$ FOR OUTPUT AS #3
90 WHILE EOF(1)<>-1
110 INPUT#1, ONE
120 INPUT#2, TWO
130 WRITE#3, ONE, TWO
140 WEND
150 STOP
```

## APPENDIX D. PROGRAM TO PERFORM RESISTIVITY CALCULATION

```
10 REM PROGRAM TO CALCULATE THE RESISTIVITY
30 REM USING THE SAMPLE'S RESISTANCE, AREA, AND LENGTH
50 INPUT "WHAT IS THE INPUT DATA FILE NAME"; INPUTFILENAME$
60 INPUT "WHAT IS THE OUTPUT DATA FILE NAME";
OUTPUTFILENAME$
65 OPEN INPUTFILENAME$ FOR INPUT AS #1
70 OPEN OUTPUTFILENAME$ FOR OUTPUT AS #2
80 INPUT "WHAT IS THE WIDTH IN METERS";W
90 INPUT "WHAT IS THE HEIGHT IN METERS"; H
100 INPUT "WHAT IS THE LENGTH IN METERS"; L
150 WHILE EOF(1)<>-1
160     INPUT#1, T,R
165 REM MULTIPLY RESISTIVITY BY 1E9 TO ALLOW GRAPHING OF
WHOLE NUMBERS
170     RO=1E+09*R*W*H/L
190     WRITE#2, T,RO
200 WEND
210 STOP
```

## APPENDIX E. PROGRAM TO CALCULATE KSTAR

```
REM PROGRAM TO CALCULATE ln K* AT GIVEN T
REM INPUTS ARE DELTA Cp, T, INCREMENTAL AREA (a),
REM TOTAL AREA (A), AND HEATING RATE Q
REM EQUATION USED:  K*=(Q(Cp tan - Cp)/(A - a))*(H/(K*T))
CLS
INPUT "ENTER FILENAME FOR OUTPUT ", FILENAME$
OPEN FILENAME$ FOR OUTPUT AS #1
CLS
INPUT "ENTER HEATING RATE IN DEGREES K PER MINUTE ", Q
CLS
INPUT "ENTER TOTAL AREA UNDER CURVE IN kJ/kg", A
CLS
INPUT "ENTER TOTAL WEIGHT IN GRAMS", W
CLS
INPUT "CONVERSION FOR CHART, CM PER 5 UNITS (Y AXIS)", C
CLS
h = 6.626E-34    'PLANCKS CONSTANT (J*s)
k = 1.381E-23    'BOLTZMANS CONSTANT (J/K)
CalToJoule = 4.187
SEC = 60         'CONVERT MINUTES TO SECONDS
CHART = .0012    'CONVERT DSC CHART UNITS TO mcal/s FOR DSC
RANGE = 10, CHART RECORDER = 20
CHARTBLOCKS = 5 'MEASUREMENTS ARE FOR 5 CHART BLOCKS

LPRINT "T", "LnKstar"
Cptan = 1
WHILE Cptan = 1
        PRINT "TO END PROGRAM ENTER NEGATIVE VALUE FOR Cp
FROM TANGENT LINE."
        INPUT "ENTER -1 TO END PROGRAM, 1 TO CONTINUE ",
Cptan
        IF (Cptan < 0) THEN END
        CLS
        INPUT "ENTER DELTA Cp IN CM ", Cp
        CLS
        INPUT "ENTER TEMPERATURE ", T
        CLS
        INPUT "ENTER INCREMENTAL AREA ", Aa
        Kr = ((Q * CHART * CalToJoule * CHARTBLOCKS) / (C *
W)) * (Cp / (SEC * (A - Aa)))
        Kstar = (Kr * h) / (k * T)
        X = LOG(Kstar)
        LPRINT T, X
        WRITE #1, X, T
```

```
        CLS
WEND
STOP
```

## APPENDIX F. PROGRAM TO CALCUATE THERMODYNAMIC QUANTITIES

```
CLS
ANSWER$ = "Y"
WHILE ANSWER$ = "Y"
CLS
INPUT "ENTER FILENAME WITH DATA ", FILENAME$
OPEN FILENAME$ FOR INPUT AS #1
R = .308          'GAS CONSTANT
h = 6.626E-34     'PLANCKS CONSTANT J*S
k = 1.381E-23     'BOLTZMANS CONSTANT J/K
LPRINT FILENAME$
LPRINT "T", "EA", "DELTAH", "DELTAS", "DELTAG"

WHILE EOF(1) <> -1
        INPUT #1, LNKR, T, SLOPE
        KR = EXP(LNKR)
        EA = R * T * T * SLOPE
        DELTAH = EA - (R * T)
        DELTAS = DELTAH / T + (R * LOG((h * KR) / (k * T)))
        DELTAG = -(R * T) * LOG((h * KR) / (k * T))
        LPRINT T, EA, DELTAH, DELTAS, DELTAG
WEND
CLOSE #1
CLS
INPUT "RUN AGAIN? (Y/N) ", ANSWER$
IF ANSWER$ = "y" THEN ANSWER$ = "Y"
WEND
STOP
```

## LIST OF REFERENCES


1. Hunt, M., "Aluminum Composites Come of Age", Materials Engineering, Vol. 106, pp. 37-40, January 1989.

2. Rack, H. J. and Krenzer, R. W., "Thermomechanical Treatment of High Purity 6061 Aluminum", Metallurgical Transactions A, Vol. 8A, pp. 335-346, February 1977.

3. Nieh, T. G. and Karlak, R. F., "Aging Characteristics of $B_4C$-Reinforced 6061-Aluminum", Scripta Metallurgica, Vol. 18, No. 1, p. 25, 1984.

4. Christman, T. and Suresh, S., "Effects of SiC Reinforcements and Aging Treatments on Fatigue Crack Growth in an Al-SiC Composite", Materials Science and Engineering A, Vol. 102, pp. 211-216, 1988.

5. Suresh, S., Christman, T. and Sugimura, Y., "Accelerated Aging in Cast Al Alloy - SiC Particulate Composites", Scripta Metallurgica, Vol. 23, pp. 1599-1602, September 1989.

6. Dutta, I. and Bourell, D. L., "A Theoretical and Experimental Study of Aluminum Alloy 6061-SiC Metal Matrix Composite to Identify the Operative Mechanisms for Accelerated Aging", Materials Science and Engineering, Vol. A112, pp. 67-77, 1989.

7. Papazian, J. M., "Effects of SiC Whiskers and Particles on Precipitation in Aluminum Matrix Composites", Metallurgical Transactions A, Vol. 19A, pp. 2945-2953, December 1988.

8. DeMeis, R., "New Life for Aluminum", Aerospace America, Vol. 27, No. 3, March 1989.

9. Osamura, K. and Ogura, T., "Metastable Phases in the Early Stage of Precipitation in Al-Mg Alloys", Metallurgical Transactions A, Vol. 15A, pp. 835-842, May 1984.

10. Gaskell,David R., Introduction to Metallurgical Thermodynamics, McGraw-Hill Book Co., 1973.

11. DeIasi, R. and Adler, P. N., "Calorimetric Studies of 7000 Series Aluminum Alloys: I. Matrix Precipitate Characterization of 7075", Metallurgical Transactions A, Vol. 8A, pp. 1177-1183, July 1977.

12. Adler, P. N. and DeIasi, R., "Calorimetric Studies of 7000 Series Aluminum Alloys: II. Comparison of 7075, 7050, and RX720 Alloys", Metallurgical Transactions A, Vol. 8A, pp. 1185-1190, July 1977.

**INITIAL DISTRIBUTION LIST**

| | | No. Copies |
|---|---|---|
| 1. | Defense Technical Information Center<br>Cameron Station<br>Alexandria, Virginia 22304-6145 | 2 |
| 2. | Library, Code 0142<br>Naval Postgraduate School<br>Monterey, California 93943-5002 | 2 |
| 3. | Professor I. Dutta<br>Department of Mechanical Engineering<br>Naval Postgraduate School<br>Monterey, California 93943-5004 | 6 |
| 4. | Research Administration, Code 012<br>Naval Postgraduate School<br>Monterey, California 93943-5000 | 1 |
| 5. | J. Hafley<br>111 David's Way<br>Yorktown, Virginia 23692 | 2 |
| 6. | Department Chairman, Code 69 HY<br>Department of Mechanical Engineering<br>Naval Postgraduate School<br>Monterey, California 93943-5000 | 1 |
| 7. | Naval Engineering Curricular Office, Code 34<br>Naval Postgraduate School<br>Monterey, California 93943-5000 | 1 |
| 8. | Dr. Alan S. Edelstein<br>Code 6371<br>Naval Research Laboratory<br>Washington, D.C. 20375-5000 | 1 |